

# Field-Circuit Model of the Resistive Welding Load and the Welding Power Source for Reducing Power Consumption and Electromagnetic Noise.

L. Sakhno<sup>1)</sup>, O. Sakhno<sup>1)</sup>, S. Dubitsky<sup>2)</sup>

<sup>1)</sup>St. Petersburg State Polytechnic University, Department of Theoretical Electroengineering,  
<sup>2)</sup>Tor Ltd, St. Petersburg Russia.

**Abstract** — Resistance welding machines with inverter power sources are considered. The equivalent scheme of the welding load for resistance butt flash welding is proposed, which based on the experimental analysis of physical processes in the flashing zone. The model was used for the AC analysis of the input current and the welding circuit in application to the inverter power unit for a steel pipe flash butt welder. The equivalent circuit of the three-winding transformer is proposed, where the primary and secondary windings are coupled by the coefficient of mutual induction on the leakage flux. Self and mutual leakage inductances of the transformer are calculated and optimized by means of 2D FEA simulation. Electromagnetic processes in welding machines are modeled in time domain with P-Spice simulation.

The above model was used for optimization of the inverter based welding power supply. The results of time domain simulation of the welding power source were confirmed experimentally.

**Keywords** — electromagnetic compatibility, power consumption, resistance welding machine, transformer leakage inductance, short-circuit resistance.

## I. INTRODUCTION

At present, most welding machines have power supplies of industrial frequency. At the same time, work is underway to create inverter power sources and expand their production. The world's leading global manufacturers of the welding equipment have such machines in their product line.

Electric welders represent a common source of electromagnetic noise in power networks. Such noise stems from a nonlinear and asymmetric load of power networks with the welders in operation, which results in distortion of their current and voltage curves. Moreover, an abruptly non-uniform power intake from the network or a limited power source (diesel generator) is possible in welding, and inducing voltage drops. The electromagnetic noise may deteriorate the quality of electric power. What is why most industrial welders are generally powered by autonomous networks equipped with noise suppression devices. Voltage drops at the power source buses adversely affect welder's operation, because high-quality

welds can be obtained only with a stable voltage at the welder's input. The voltage drops can also upset serviceability of the welder having an inverter power unit. Hence, development of new welders entails evaluation of their impact on supply network or diesel generator and necessitates provision of their electromagnetic compatibility.

The block diagram of an inverter source with rectifier consists of the three-phase bridge rectifier with the capacitor filter, the inverter, and the welding transformer. The secondary windings are loaded with a welding arc via the single-phase center-tapped full-wave rectifier (Fig.1).

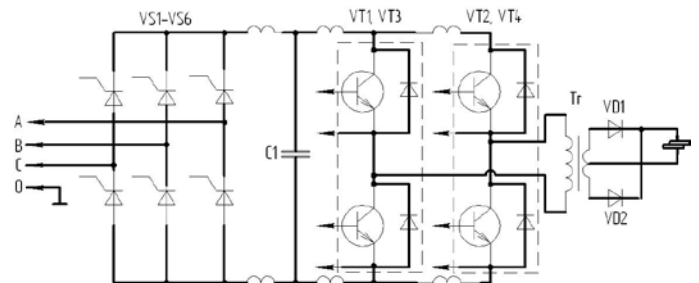


Fig. 1. Block diagram of the power source for a resistance welding machine.

Frequency of the inverter is identified by both requirements of quality welding and the demands of minimizing the weight and size of the transformer. A number of technical problems should be resolved to create the reliable inverter power source. One of problems is the development of the welding transformer, which influences in great extent on the overall power consumption.

## II. CALCULATION OF POWER CONSUMPTION

The power consumed by a welding machine is defined by the following formula:

$$S = U_1 I_1 \approx U_2 I_W, \quad (1)$$

where  $U_1$  – actual value (rms) of the voltage source to which the primary winding is connected,  $I_1$  – rms of current in the primary winding,  $U_2$  – the rms of idle run voltage of the

secondary winding,  $I_W$  – rms of the welding current.

The load voltage of the welding transformer depends on the welding current, the volt-ampere characteristic of the welded zone, and the short-circuit impedance of the transformer:

$$U_2 = I_W z. \quad (2)$$

The impedance  $z$  in (2) has two following components:

$$z = z_{SC} + z_{LOAD}, \quad (3)$$

where  $z_{SC} = r_{SC} + ix_{SC}$  – the short-circuit impedance of the transformer referred to the secondary winding,  $r_{SC}$ ,  $x_{SC}$  – the resistance and reactance of the transformer referred to the secondary winding,  $i = \sqrt{-1}$ ,  $z_{LOAD}$  – impedance of welding arc.

The welder's load is a welding circuit which represents a number of rigid and flexible conductors connecting the secondary winding to the welder's electrodes between which the parts to be welded are placed. The equivalent circuit thus comprises the inductances and resistances for secondary circuit, electrodes, sections of welded parts, through which welding current passes.

Thus, the short-circuit resistance  $z_{SC}$  and resistance of welder's load  $z_{LOAD}$  affects on the calculated value of idling, and consequently, the power consumption of the welder.

### III. EQUIVALENT CIRCUIT OF RESISTANCE FLASH WELDER'S LOAD

The load of resistance welder consists of active resistance of the current leads from the secondary windings of the transformer to the welding electrodes and welded details (in range 100...200  $\mu\Omega$ ).

The load of resistance butt flash welder involves parts preheated to a near-melting temperature and the nonlinear components simulating the flashing zone in welding. In development of an equivalent load circuit selection of such components presents a major difficulty because of complexity of physical processes in the flashing zone [1]. Let us consider features of the flashing process with the view to replace the flashing zone with electric circuit components. On account of a high density of current at elementary contacts between parts, they heat up and convert to liquid straps on coming in contact with each other. Changes in the volume and shape of the liquid straps are due to metal melting, movement of the strap over the surface of parts, its compression by electrodynamic forces, and liberation of vapors and gases out of the overheated metal volume. Such phenomena are responsible for abrupt changes in resistance of the flashing zone. Disintegration of liquid metal straps occurs under the influence of electrodynamic forces and metal overheating. Such disintegration is accompanied by arcing with constant voltage maintained at the flashing zone and the welding current dropping to zero. Experiments show that resistance at the flashing zone undergoes three-four-fold changes. Frequency of changes in resistance and arcing may range from 500 Hz to a few kHz, and arcing duration accounts for several tens of microseconds.

With stable flashing, the welding current curve is not strictly cyclical, but, considering its recurrent nature in each cycle (both for the envelope curve and for single-pulsation currents), the welding current curve may be regarded cyclical for analysis of phenomena with an averaging interval of about 0.1 s, the cycle being equal to that of supply voltage. The flashing process generally takes tens of seconds and involves several stages. The first stage can be close to the welder's short-circuit or a no-load condition caused by the slopping of the metal from the flashing zone thank to electrodynamic forces. The second stage starts when the arc establishes. Their role depends on the properties of the flashed material and the flashing condition. At the last stage, when the film of molten metal forms on the surface of welded parts, these are pressed up together, which corresponds to the welder's short-circuit. The duration of that stage is 0.1 to 0.8 s. The basic parameters of the flashing condition, such as the equivalent contact resistance, the number of connections and disconnections for the flashed butts per unit time, and the voltage at the flashing zone in arcing, only obtained experimentally for various materials and cross-sections of the welded parts.

Complying with the above stages of the welding process, the equivalent circuit for the flashing zone should fit the following load conditions:

- the short-circuit condition;
- the no-load condition,
- transition from the no-load condition to the short-circuit condition, describing the initial flashing stage,
- step-type changes in resistance of the flashing zone,
- the cycling arcing.

On various welding stages, the flashing zone is simulated either by a given resistance or by a constant electromotive force (emf).

The first of the above conditions reflects the contact occurrences at the flashing zone, and the second, the arc phenomena. When the diode valve is closed, the resistance or the emf source are disconnected from the welder's load; when it is opened, they are connected to the load.

The mathematical model was developed to analyze electromagnetic compatibility for welders, the load of which was given above. The model allows simulating of important electromagnetic processes to obtain the harmonic spectrum of currents and voltages in any component of welder circuit with various rectifier configurations and in wide range of power and frequency.

### IV. THE EQUIVALENT CIRCUIT OF A THREE – WINDING TRANSFORMER

The inverter power source in fig.1 uses a three-winding transformer. An example of such a transformer with disk alternating windings is shown in fig.2. The primary winding consists four coils connected in series and wound by a rectangular cooper wire. The two secondary coils are made of copper tubes through which cooling water flows. Figure 2 shows the numbers of coils, the thickness of the coil of the

primary winding  $b$  and the size  $c$  of the wire of the coil. For the basic transformer the thickness of the coil  $b = 5$  mm, the size  $c = 1,6$  mm.

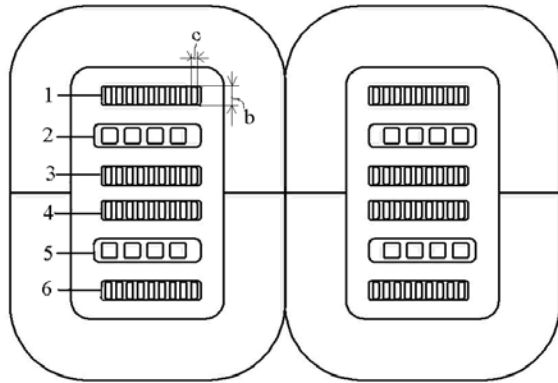


Fig.2. Design of the transformer with four primary coils

The equivalent circuit of three-winding transformer [7] is shown in fig.3. The main difference between the proposed equivalent circuit and the well-known one is that the windings are electrically insulated, and always have positive inductances. Therefore, the circuit is suitable for the standard P-Spice circuit simulation software [6]. It is very important that the circuit parameters have clear physical sense and can be easily evaluated by FEA [2], [4] by calculation the energy of magnetic field divided to squared current.

This circuit is based on replacing the three-winding transformer with two transformers: one with windings 1, 2 and the second with windings 1, 3 (further denoted as transformers 1-2 and 1-3). The mutual impact of transformers 1-2 and 1-3 is modeled as a change of EMF on the terminals of their secondary windings due to magnetic leakage fields. The degree of magnetic coupling of these transformers is characterized by the magnetic coupling factor of the leakage fluxes  $k = \frac{M}{\sqrt{L_{12}L_{13}}}$  ( $L_{12}$  and  $L_{13}$  - the leakage inductances of

the transformers 1-2 and 1-3 referred to their secondary sides,  $M$  - the mutual inductance of the leakage fluxes).

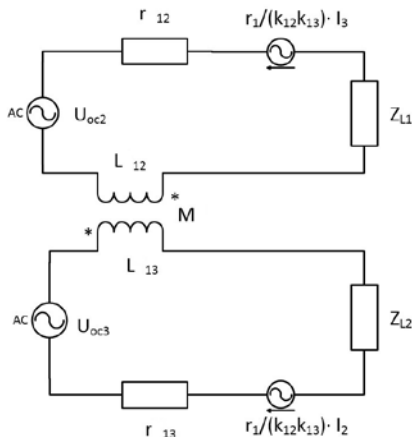


Fig.3. Equivalent circuit of three-winding transformer

The magnetic coupling factor  $k$  is convenient for the

analysis of the transformer design influence on the power consumption. If  $M > 0$  the direction of the leakage flux in winding 3 caused by transformer 1-2, is opposite to the direction of the main magnetic flux in this winding. If  $M < 0$  the leakage flux and the main flux in winding 3 have the same direction. Similarly, if  $M > 0$  the direction of the leakage flux in winding 2 caused by transformer 1-3 is opposite to the direction of the main magnetic flux in this winding. If  $M < 0$  the leakage flux and the main flux have the same direction. In the equivalent circuit in fig.2  $r_{12}$ ,  $r_{13}$  are resistances of transformers 1-2 and 1-3 referred to the secondary side,  $z_{L1}$ ,  $z_{L2}$  are secondary load impedances. We also introduce dependent sources of EMF  $\frac{r_1}{k_{12}k_{13}}I_2$  and  $\frac{r_1}{k_{12}k_{13}}I_3$  ( $r_1$  is an resistance of the primary winding,  $k_{12}$  and  $k_{13}$  are the transformation ratios). They take into account the change of the voltage at the terminals of the winding 3 and 2 due to a primary winding voltage drop of the transformer 1-3 and 1-2. The magnetic leakage fields in transformers 1-2, 1-3 (short-circuit tests for transformers 1-2, 1-3) was modelled by 2D FEA software QuickField [5]. From the FEA model we evaluate parameters  $L_{12}$ ,  $r_{12}$ ,  $L_{13}$ ,  $r_{13}$  in the equivalent circuit. For evaluating the magnetic leakage mutual inductance  $M$  we made the FEA simulation of another short-circuit field in transformer 2-3. For simulation of electromagnetic processes in the scheme in fig.1 the P-Space [6] Microcap software was used.

### V. THE RESULTS OF TRANSFORMER OPTIMIZATION

For further analysis we choose the transformer with disk alternating windings (Fig.2).

For ease of analysis, the results of calculation of the short circuit resistance are presented in relative units. When observing the leakage inductance, relative inductance  $L = \frac{L'_{SC}}{L'_0}$  is considered, where  $L'_{SC}$  - leakage inductance given to the primary winding  $L'_0$  - the DC leakage inductance related to the primary winding.

Let us also introduce the relative resistance:  $R = R_j/R_{0j}$  where  $R_j$  is the AC resistance of the j-th coil,  $R_{0j}$  - its DC-resistance,  $R_a = R_j/R_a$  is the ratio of the AC-resistance of the j-th coil to resistance to the DC-resistance of a coil with the same width and the height equal to the penetration depth  $a = \sqrt{2/\omega\mu\gamma}$  by the given frequency.

Relative resistance  $R$  allows us to estimate the supplementary losses in the each coil. Relative resistance  $R_a$  at constant values of  $\omega, \mu, \gamma$ , which is proportional to the resistance  $R_j$ , allows us to investigate in relative units the dependence of the resistance of the coil on its thickness  $b$ , i.e. to investigate the degree of copper utilization in the coil. The minimum of the function  $R(b)$  gives the critical thickness of

the winding, increasing of which leads to an increase rather than a decrease of losses at a given frequency.

Relative leakage inductance of the transformer  $L$  decreases with an increase of the frequency due to skin effect. At a frequency of 10 kHz, this decrease is approximately 30% (Fig.4). Therefore, due to the skin effect the leakage reactance increases slowly than proportional to the frequency.

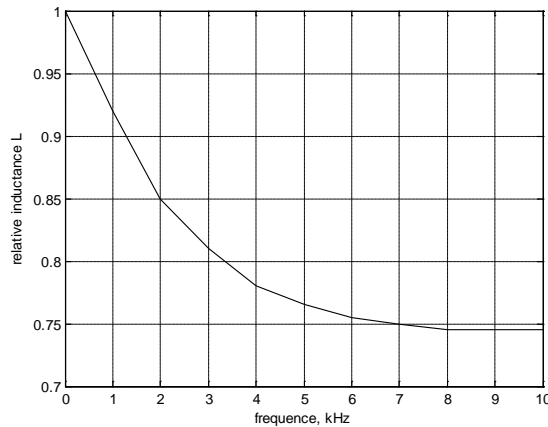


Fig.4. Dependence of relative inductance of the transformer

The winding resistance also increases with the frequency due to skin effect. Figure 5 shows the resistance vs. frequency dependence in relative units.

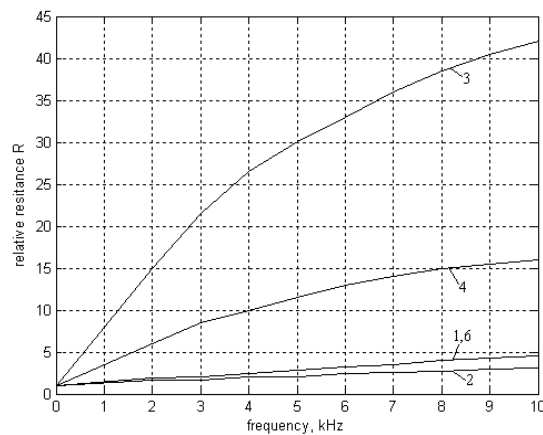


Fig.5. Dependence of relative resistances of the coils on frequency

We can conclude that the maximum of supplementary losses locates in the coil 3 of the primary winding. For example, at a frequency of 10 kHz value of relative resistance of the coil 3 exceeds about 40 while for the coil 1 and 6 its value is about 5. This difference is explained by fact that coil 3 is located in a stronger magnetic leakage field. In turn, the leakage field is non-uniform because during each half-period only one of two secondary coils is energized. Large supplementary losses in coils 3 and 4 lead to a sharply expressed minimum in the dependence of relative resistance  $Ra$  vs. the coil thickness. As an example in fig.6, dependence of relative resistance  $Ra$  on coil thickness at a frequency of 10 kHz is given. This figure shows that the critical thickness of coil 3 is about 0.8 mm, and of the coil 4 - about 1.0 mm.

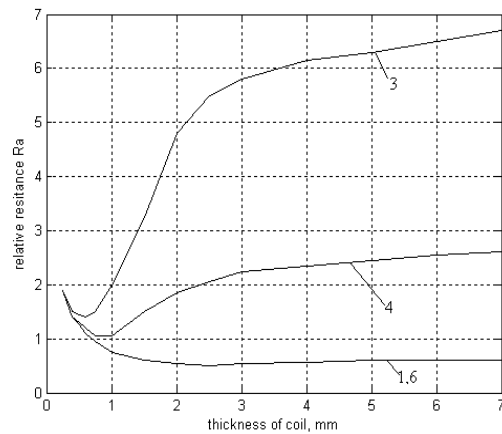


Fig.6. Dependence of the relative resistances of the coils on coil thickness

Therefore, at 10 kHz and the thickness of the coil  $b = 5$  mm there will be an excessive consumption of copper in these coils. It should be noted that for coils 1 and 6 (Fig. 2), in which supplementary losses are significantly less, than in coils 3 and 4, the increasing of thickness of the coil  $b$  have no significantly effect on the AC resistance of the coil. For coils 3 and 4 even a small deviation from critical thickness leads to a sharp increase of its resistance and an excessive consumption of copper.

FEA simulation shows that the maximum supplementary losses are located in the central coils of primary winding. A slight deviation of the thickness of primary winding coil from the critical value at frequencies above 1 kHz leads to a large increase of the supplementary losses.

In order to reduce of supplementary losses in the primary winding and its leakage reactance in high frequency range it is suggested to change the coil arrangement. We compared two different transformer design: with three (fig. 7) and two (fig. 8) primary coils. Both arrangements have the same cross-section area of the window.

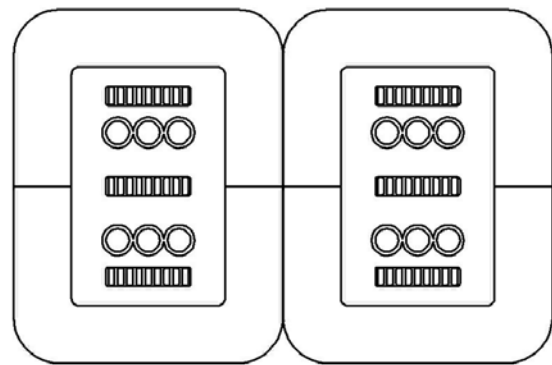


Fig.7. Transformer with three primary coils.

In the design in fig.8, all the turns of the primary winding are arranged in two coils. Two disks of the secondary winding are located between them. This design differs significantly

from the conventional layout of the welding transformer. This leads to essential reduction of leakage inductance of the transformer and supplementary losses in the primary winding. The relative coil resistances and the critical values of the thickness of the primary winding are defined by the curves 1 and 6 in fig.5 and 6.

The proposed design (fig.8) was implemented in a transformer for inverter power source with a rated frequency 7.5 kHz, rated welding current 6 kA. Thanks to special winding arrangement the short-circuit impedance was approximately halved. That means almost twice less consumption of the core steel, copper, and the input power.

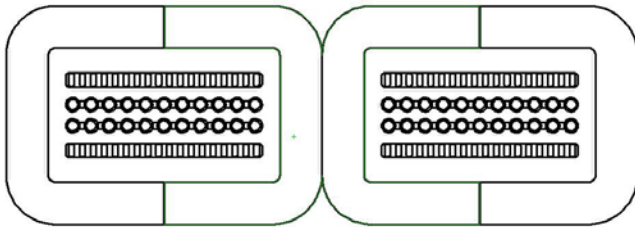


Fig.8. Transformer with two primary coils

For comparison the pattern of leakage field is shown for the conventional transformer (fig. 9) and for the optimized transformer (fig. 10)

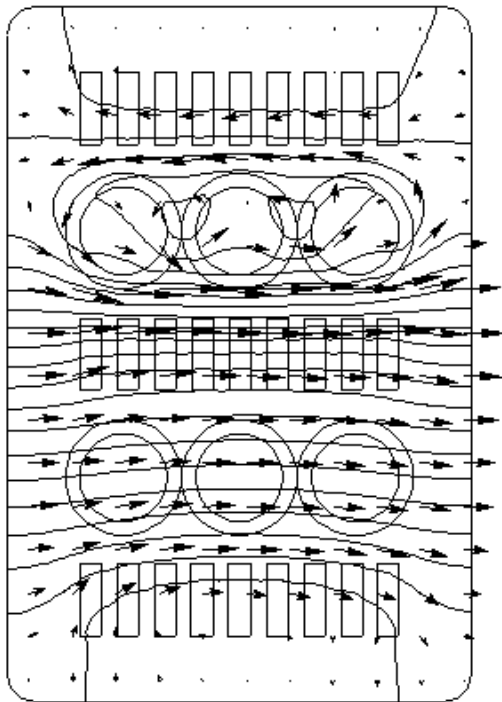


Fig. 9 Leakage field pattern of the conventional transform

Unlike the conventional design, the proposed winding layout is not very sensitive to small variation of thickness of the primary winding around its critical value.

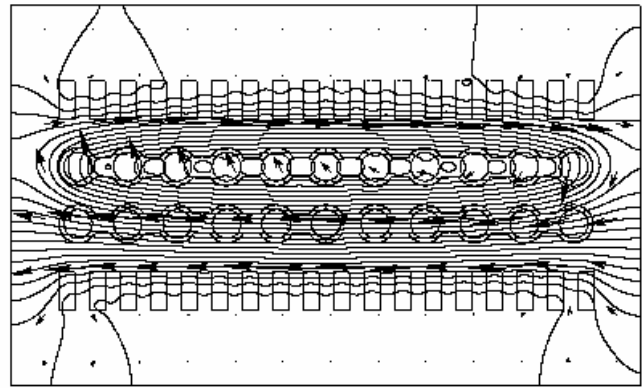


Fig. 10 Leakage field pattern of the modified transform

The measured inductance and reactance of the transformer differ from theoretically predicted values in less than 10%.

#### VI. ANALYSIS OF POWER CONSUMPTION AND ELECTROMAGNETIC NOISE GENERATED BY RESISTANCE FLASH WELDER

The above mathematical model of resistance flash welder's load is used to model electromagnetic processes in the welding power source with thyristor-based inverter. The studied welding machine is designed for welding the large-diameter gas and oil pipeline. Unlike the scheme on fig. 1, this power source has no rectifier in the welding circuit. The welding machine is powered by the transformer with rated power 650 kVA, the secondary voltage 380 V, and the length of current-carrying wires from the welder to the transformer of about 100 m.

The power source is rated at 250 kVA, the inverter frequency ranges from 50 Hz to 100 Hz, and the rectifies voltage is 400-430 V. The capacitance of the capacitor bank varies from 25,000 to 75,000  $\mu\text{F}$ . Our goal is analyzing the influence of the flashing butt welders to the enterprise electric network.

We have simulated all the consequence welding stages. During the welding cycle the total input power varies by a factor of 3.2.

Simulation shows that the variation of phase input currents is up to 17% with 30,000  $\mu\text{F}$  filter capacitance, or up to 10% with 75,000  $\mu\text{F}$  filter capacitance. Momentary voltage surges caused by variations in the welder's load, observed as high as 60 V. The voltage distortion factor is about 16% with 50,000  $\mu\text{F}$  filter capacitance and up to 15% with 75,000  $\mu\text{F}$ .

We compared the simulation results with measured data. Voltages and currents were recorded by mirror-galvanometer oscillographs, ohmmeters, voltmeters, and wattmeters. The measured and simulated data are in agreement good enough for accurate predicting of voltage drop, input power and welding current. The inverter based power source provides the uniform power consumption by all three phases, but does not actually reduce the non-uniformity of power consumption during the welding cycle.

## VII. CONCLUSION

The presented mathematical model allows to estimate the load asymmetry, non-uniformity of power consumption during welding stages, the distortion of currents and voltages in any circuit component, and the overall power consumption.

The equivalent circuit of the flashing zone of welded parts is proposed. It is based on large amount of experimental data of recorded welding current and voltage.

The simulated electromagnetic behavior was confirmed by measured data obtained from the inverter power source of steel pipe flash welders.

The proposed mathematical model is suitable for optimization of the welding transformer. It allowed us to propose the new design of transformer that reduced the overall power consumption approximately twice. The above result was confirmed experimentally.

## REFERENCES

- [1] Bradáč J. Determination of Parameters of EVP Material Model in Numerical Welding Simulations //WSEAS Transactions on Applied & Theoretical Mechanics. – 2013. – T. 8. – №. 3.
- [2] Cârstea D., Cârstea A. A., Cârstea I. Coupled electromagnetic, thermal and stress analysis of large power electrical transformers //Proceedings of the 9th WSEAS International Conference on International Conference on Automation and Information. – World Scientific and Engineering Academy and Society (WSEAS), 2008. – C. 29-34.
- [3] Al-Bahadly I., Saffar M. Resonant Converter Power Supply for Arc Welding Application //Proceeding of the 5th WSEAS International Conference on Power Systems and Electromagnetic Compatibility, Greece. – 2005. – p. 269-273.
- [4] Kashtiban A. M., Milani A. R., Haque M. T. Finite element calculation of winding type effect on leakage flux in single phase shell type transformers //Proceedings of the 5th WSEAS international conference on Applications of electrical engineering. – World Scientific and Engineering Academy and Society (WSEAS), 2006. – C. 39-43.
- [5] Claycomb J. R. Applied Electromagnetics Using QuickField and MATLAB. – *Laxmi Publications, Ltd.*, 2010.
- [6] A. Vladimirescu The SPICE Book, *John Wiley & Sons, Inc.*, First Edition, 1994W.-K. Chen, *Linear Networks and Systems* (Book style). Belmont, CA: Wadsworth, 1993, pp. 123–135.
- [7] L. Sakhno, O. Sakhno, S. Dubitsky Field-Circuit Modelling of an Advanced Welding Transformer with Two Parallel Rectifiers. – XXIII Symposium Electromagnetic phenomena in nonlinear circuits. 2-4 July, 2014, University of West Bohemia, Pilsen, Czech Republic, 2014, pp. II-17/33-34

**Lyudmila Sakhno** is a professor of electromagnetic theory in St. Petersburg polytechnic University, She has graduated from the same university in 1974 In 2006 she earns the of Doct. Techn. Sci. degree. Dr. L. Sakhno worked for many years with the research institute for welding equipment in Leningrad. Her doctor dissertation is devoted to theoretical analysis and optimization of welding transformers with multiple windings.

**Olga Sakhno** graduated from the the Leningrad Polytechnical Institute in 1974 In 1983 she received the degree of Candidate Techn. Sci (analog of the PhD degree) from the LPI. Her thesis dealt with the analysis and development of theoretical methods for calculation electromagnetic processes in electric network. She is a lecturer at Department of Mathematics of St. Petersburg State Polytechnic University.

**Simon Dubitsky** is currently with Tor Ltd, St. Petersburg. He receives MsC degrees in electrical engineering in 1983 and in computer science in 2003 both from SPbSPU. His main area of activity is development of QuickField FEA software in cooperation with Tera Analysis company locates in Svendborg, Denmark. Main research interest is implementing FEA as a handy tool for everyday engineering practice, advanced postprocessing of electromagnetic field solution, multiphysics FEA analysis coupled with circuit equations and surrogate models.